

# Mechanistic Aspects of the Selective Reduction of NO by Propene over Alumina and Silver–Alumina Catalysts

F. C. Meunier,<sup>1,2</sup> J. P. Breen,<sup>1</sup> V. Zuzaniuk, M. Olsson, and J. R. H. Ross

*Centre for Environmental Research, University of Limerick, Limerick, Ireland*

Received April 28, 1999; revised June 28, 1999; accepted June 28, 1999

The selective catalytic reduction of NO with C<sub>3</sub>H<sub>6</sub> in the presence of a large excess of O<sub>2</sub> (i.e., C<sub>3</sub>H<sub>6</sub>-SCR (selective catalytic reduction)) was studied over  $\gamma$ -Al<sub>2</sub>O<sub>3</sub>, 1.2% Ag/ $\gamma$ -Al<sub>2</sub>O<sub>3</sub>, and 10% Ag/ $\gamma$ -Al<sub>2</sub>O<sub>3</sub> catalysts. The  $\gamma$ -Al<sub>2</sub>O<sub>3</sub> and the low-loading silver material exhibited high conversions to N<sub>2</sub> whereas the high-loading sample predominantly yielded N<sub>2</sub>O. Surprisingly, a comparison of actual NO<sub>2</sub> yields to thermodynamically predicted yields of NO<sub>2</sub> showed that the formation of NO<sub>2</sub> during the C<sub>3</sub>H<sub>6</sub>-SCR of NO over  $\gamma$ -Al<sub>2</sub>O<sub>3</sub> was not achieved through the direct oxidation of NO with O<sub>2</sub>. An alternative mechanism involving the formation of organo-nitrite species followed by their decomposition/oxidation was suggested to be the main route for the formation of NO<sub>2</sub>. The promoting role of low loadings of silver on alumina on the activity for N<sub>2</sub> production was attributed to the higher rate of formation of inorganic ad-NO<sub>x</sub> species (e.g., nitrates) as evidenced by *in situ* DRIFTS and thermogravimetric analyses. It was proposed that these inorganic ad-NO<sub>x</sub> species further react with the reductant or a derived species to form various organo-NO<sub>x</sub> compounds. In particular, organo-nitro and organo-nitroso compounds and/or their derivatives (e.g., isocyanate, cyanide, amines, and NH<sub>3</sub>) were suggested to react with NO or the organo-nitrite and/or its derivative NO<sub>2</sub> to yield N<sub>2</sub>. When no reductant was present, the low-loading Ag/ $\gamma$ -Al<sub>2</sub>O<sub>3</sub> material was poisoned by strongly bound nitrates and its activity for NO<sub>2</sub> formation was similar to that observed over the alumina.

© 1999 Academic Press

**Key Words:** NO; NO<sub>2</sub>; propene; silver; alumina; DRIFTS; de-NO<sub>x</sub>; reaction mechanism.

## 1. INTRODUCTION

In spite of much research work over the last 10 years or so (1, 2), the selective catalytic reduction (SCR) of NO with light hydrocarbons or oxygenated molecules is not yet a practical method to control NO<sub>x</sub> emissions in the presence of a large excess of oxygen. This failure is probably related to the complexity of the reaction mechanisms involved

<sup>1</sup>To whom correspondence should be addressed: Fax: +353-61-202602. E-mail: John.Paul.Breen@ul.ie. Fax: +49-89-289-13544. E-mail: meunier@thor.tech.chemie.tu-muenchen.de.

<sup>2</sup>Current address: Technische Universität München, D-85748 Garching, Germany.

which hinders the development of improved materials in terms of activity, selectivity, hydrothermal stability, and sulphur resistance. Burch *et al.* have contributed to the elucidation of the mechanism of the SCR reaction over Pt/Al<sub>2</sub>O<sub>3</sub> materials; in particular, the different effect of using propene or propane on the reaction pathways has clearly been established (3, 4). With propene, the surface of the platinum is kept reduced and a decomposition-type mechanism occurs on the noble metal, leading to the formation of significant amounts of N<sub>2</sub>O along with N<sub>2</sub>. With propane, the surface of the noble metal is covered with oxygen species which favours the oxidation of NO to NO<sub>2</sub> and/or ad-NO<sub>x</sub> species which subsequently react with the reductant over the alumina, selectively yielding N<sub>2</sub> (the so-called “NO<sub>2</sub> route”). The latter route underlines the importance of the alumina, in the selective reduction reaction scheme, which is not merely a support for the platinum but also participates directly in the reduction reaction.

Alumina is one of the most active single-metal oxides for the C<sub>3</sub>H<sub>6</sub>-SCR of NO and can be further promoted by a wide range of metal oxides such as cobalt (5), copper (6), or silver (7). The exact role of these compounds on the enhancement of the catalytic activity of the alumina is not trivial. In the case of Co/Al<sub>2</sub>O<sub>3</sub>, it has been suggested that the role of the promoter is to oxidise NO with O<sub>2</sub> to form NO<sub>2</sub> which subsequently reacts with the alkene on the alumina to yield N<sub>2</sub> (5, 8). This reaction mechanism would thus be similar to the NO<sub>2</sub> route observed over Pt/Al<sub>2</sub>O<sub>3</sub> in the case of the C<sub>3</sub>H<sub>8</sub>-SCR of NO. This assumption relies mostly on the fact that (1) over the alumina, the C<sub>3</sub>H<sub>6</sub>-SCR of NO<sub>2</sub> to N<sub>2</sub> proceeds much faster than that of NO and (2) the C<sub>3</sub>H<sub>6</sub>-SCR of NO<sub>2</sub> over alumina proceeds much faster than the C<sub>3</sub>H<sub>6</sub>-SCR of both NO and NO<sub>2</sub> over the Co-promoted sample. However, other results published on the oxidation of NO to NO<sub>2</sub> over Co/Al<sub>2</sub>O<sub>3</sub> materials apparently contradict this view (9). The measured activity for NO oxidation to NO<sub>2</sub> was found to be too low to be able to account for the related SCR activity. It has been suggested that the deactivation of the catalyst by strongly bound surface nitrates is possible when no reductant is available (10). The work by Yan *et al.* also stresses the importance of various phases of

cobalt species present on the alumina-based material (e.g., oxidic particles of different sizes, cobalt aluminate, and isolated  $\text{Co}^{2+}$  species).

The  $\text{Ag}/\text{Al}_2\text{O}_3$  materials seem to exhibit a different behaviour as compared to that of the  $\text{Co}/\text{Al}_2\text{O}_3$  catalysts. For the latter, increasing the cobalt content, on one hand, only favours the nonselective combustion of the reductant. On the other hand, the use of increasing contents of silver on the alumina seems also to favour a different route for the reduction, with greater proportions of  $\text{N}_2\text{O}$  being formed along with  $\text{N}_2$  (11). A similar trend has been observed on  $\text{Ag}/\text{TiO}_2\text{-ZrO}_2$  materials (12). Bethke and Kung have also reported a synergistic effect between the  $\text{Al}_2\text{O}_3$  and the  $\text{Ag}/\text{Al}_2\text{O}_3$  catalysts (11). They have postulated the existence of a short-life intermediate going from one phase to the other. In the same work, differences in the nature of the catalysts have been noticed, depending on the silver content. Under reaction conditions, metallic silver particles are thought to prevail on a 6%  $\text{Ag}/\text{Al}_2\text{O}_3$  catalyst whereas  $\text{Ag}^+$  species are thought to prevail on a 2%  $\text{Ag}/\text{Al}_2\text{O}_3$  sample. In the latter case, a higher dispersion and a greater interaction with the alumina would explain the stabilisation of an oxidised state of the silver (13). The parallelism to the results of Burch *et al.* for the  $\text{Pt}/\text{Al}_2\text{O}_3$  discussed above is tempting (4): one could postulate a decomposition-type mechanism over the metallic silver particles whereas the  $\text{Ag}^+$  phase would favour a  $\text{NO}_2$  route involving both the silver and the alumina phases. Over a 5%  $\text{Ag}/\text{Al}_2\text{O}_3$ , Sumiya *et al.* (14) reported that a  $\text{C}_x\text{H}_y\text{NO}_z$  compound was produced from  $\text{NO}$ ,  $\text{O}_2$ , and  $\text{C}_3\text{H}_6$  which subsequently decomposed to an isocyanate species. The isocyanate was found to react readily with  $\text{NO}$ ,  $\text{O}_2$ , and especially  $\text{NO} + \text{O}_2$  to produce  $\text{N}_2$  and carbon oxides. The authors concluded that organo- $\text{NO}_x$  compounds and isocyanate were crucial intermediates of the SCR reaction and that the rate-determining step was the formation of the isocyanate. It has been observed that the use of high calcination temperatures for some alumina-promoted catalysts was beneficial to the SCR reaction (15, 16). This effect has been assigned to the formation of aluminate phases which are less active for the total combustion of the reductant than the corresponding alumina-supported oxides (17, 18, 8).

We have recently reported unexpectedly high activity for the oxidation of  $\text{NO}$  to  $\text{NO}_2$  over (nonpromoted)  $\gamma\text{-Al}_2\text{O}_3$  during the  $\text{C}_3\text{H}_6\text{-SCR}$  of  $\text{NO}$  (19). Conversions to  $\text{NO}_2$  greater than that allowed by the thermodynamics of the reaction  $\text{NO} + \frac{1}{2}\text{O}_2 \rightleftharpoons \text{NO}_2$  could be obtained when complete consumption of the propene was achieved. This observation questions the validity of the accepted model of the SCR of  $\text{NO}$  over some alumina materials in which the  $\text{NO}_2$  is believed to be formed by  $\text{O}_2$  oxidation of  $\text{NO}$  (5, 8). On the basis of these results, we have proposed alternative SCR routes through a  $\text{NO}$  disproportionation reaction or a selective oxidation of the reductant which could explain the

$\text{NO}_2$  yield observed. To obtain more detailed information about the mechanism of the  $\text{C}_3\text{H}_6\text{-SCR}$  of  $\text{NO}$  over alumina and  $\text{Ag}/\text{Al}_2\text{O}_3$  catalysts, the present study compares the catalytic activity of alumina and two silver-based materials with low (i.e., 1.2%) and high (i.e., 10%) loading of silver and relates this to the surface species observed during *in situ* DRIFTS experiments.

## 2. EXPERIMENTAL

### 2.1. Catalyst Preparation and Characterisation

The  $\gamma\text{-Al}_2\text{O}_3$  utilised was supplied by Alcan (AA400) with a total surface area of  $148\text{ m}^2\text{ g}^{-1}$ . For the preparation of the silver-promoted materials, an appropriate amount of silver nitrate (BDH, analytical grade) was dissolved in a volume of deionised water equal to that of the porous volume of the alumina. The solutions were then deposited on the alumina by dry impregnation at room temperature. The samples were dried for 14 h at  $120^\circ\text{C}$  and then calcined at  $630^\circ\text{C}$  for 6 h in synthetic air.  $\text{N}_2$  adsorption at 77 K using a Micromeritics system was used to measure the surface area of the samples. Prior to these measurements, the samples were each outgassed for 2 h at  $200^\circ\text{C}$  under a dynamic vacuum (i.e., with a residual pressure lower than 20 Pa). Atomic absorption spectroscopy measurements were performed to determine the silver content of the catalysts. The silver loadings on the alumina are reported in wt%.

### 2.2. Catalytic Tests

A quartz flow microreactor (3-mm internal diameter) was used for the catalytic tests, the catalytic bed being held in place by quartz wool plugs. The temperature of the reaction was measured inside the reactor, just before the catalyst bed, by a thermocouple enclosed in a quartz tube. Unless otherwise stated, the temperature of the reactor furnace was reduced from 600 to  $200^\circ\text{C}$  in 50 or  $25^\circ\text{C}$  intervals, dwelling at each temperature for 1 h. The data points reported were taken 5 and 20 min before the end of the dwelling stage at each temperature. The reactant gases used were high-purity 1%  $\text{NO}/\text{He}$  (BOC), 1%  $\text{C}_3\text{H}_6/\text{He}$  (Air Products),  $\text{O}_2$  (BOC, 99.9%), and Ar (BOC 99.99%). The actual feed compositions used in each of the experiments reported in this paper are shown in the legends of the appropriate figures. An analysis of the reaction products was carried out using a Nicolet 550 FT-IR spectrophotometer fitted with a gas cell of volume  $0.22\text{ dm}^3$ . The gas cell and the lines of the system were heated at  $90^\circ\text{C}$ . The concentration of a given species was measured by integrating the peaks in selected regions of its absorbance spectrum and comparing these to a calibration curve. The integration intervals were selected to avoid, wherever possible, overlap between the different species (Table 1). However,  $\text{NO}_2$  had to be integrated in a region of the spectrum where  $\text{C}_3\text{H}_6$

TABLE 1  
Integration Regions Used for the Quantification of Gaseous Species

Molecule	NO	N <sub>2</sub> O and CO	NO <sub>2</sub> and C <sub>3</sub> H <sub>6</sub>	NH <sub>3</sub>
Peak measurement technique	area	area	area	height
Integration interval (cm <sup>-1</sup> )	1878.7–1872	2220–2100	2960–2900	931 <sup>a</sup>

<sup>a</sup> Peak extends over 940–924 cm<sup>-1</sup>.

also absorbs and these products were therefore quantified together using matrix-based calculations (QuantIR software); the same applied to the combination of N<sub>2</sub>O and CO. A relative precision better than ±2% was estimated for the measured concentrations of the different species. As N<sub>2</sub> is not IR active and hence could not be detected, its concentration was calculated assuming that there was a mass balance of 100% for all the nitrogen-containing molecules. The relative precision obtained on the value of N<sub>2</sub> was estimated to be better than 6% and therefore lower than that of the other N-containing products which were directly quantifiable. Hydrogen cyanide, which was only observed at higher temperatures over the alumina catalyst, was not quantified but this was thought to affect the N balance only to a minor extent (20). The yields were calculated on a nitrogen-atom basis, i.e., N<sub>2</sub> yield = 20%, meaning that 20% of the NO molecules was converted to N<sub>2</sub>. On one hand, blank experiment using an empty reactor showed no significant conversion of NO up to 600°C at the lowest flow rate employed (feed was 0.05% NO + 0.05% C<sub>3</sub>H<sub>6</sub> + 2.5% O<sub>2</sub>/He; total flow = 22.5 ml min<sup>-1</sup>). On the other hand, the conversion of propene was ca. 6% at this temperature.

### 2.3. Thermogravimetric Analysis

Weight changes associated with passing NO and O<sub>2</sub> over different materials were measured as a function of time using an intelligent gravimetric analyser (IGA) supplied by Hiden Analytical and capable of detecting changes in mass of ±0.1 μg. Samples of 100 mg were first annealed in a He stream of 100 cm<sup>3</sup> min<sup>-1</sup> at 450°C for 3 h. The temperature was then reduced to 400°C and the system was flushed with a 400 cm<sup>3</sup> min<sup>-1</sup> stream of 2.5% O<sub>2</sub>/He for 1 h. At this stage 500 ppm of NO was introduced into the stream and the weight changes were recorded.

### 2.4. Diffuse Reflectance FT-IR Analysis

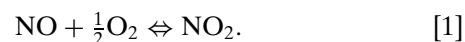
The diffuse reflectance FT-IR measurements were carried out *in situ* in a high-temperature cell (Spectra-Tech) fitted with ZnSe windows. The sample for study (ca. 30 mg) was finely ground and placed in a ceramic crucible, the temperature of which could be varied from 20 to 800°C. All the samples were calcined *in situ* at 630°C prior to analysis. The temperature of the sample was increased from room temperature in 100°C steps, dwelling at least 1 h at each

temperature. Unless otherwise stated, the spectra reported here were taken after dwelling at a given temperature for 40 min. The absorbance measured in the presence of the reaction stream over the catalyst relative to that of the same material at the same temperature under a stream of argon is reported. Usually 64 or 128 scans were recorded at a resolution of 2 cm<sup>-1</sup>. The assignments of the absorption bands reported were based on those reported in the literature and other experiments (not shown) in which the reaction of propene and NO were investigated separately in the presence of a large excess of dioxygen.

## 3. RESULTS

### 3.1. Activity of γ-Al<sub>2</sub>O<sub>3</sub> and Ag/γ-Al<sub>2</sub>O<sub>3</sub> Catalysts for the C<sub>3</sub>H<sub>6</sub>-SCR of NO

Figure 1 shows the propene and NO conversions and the yields of N<sub>2</sub>, NO<sub>2</sub>, N<sub>2</sub>O, and NH<sub>3</sub> for the title reaction over γ-Al<sub>2</sub>O<sub>3</sub> (148 m<sup>2</sup> g<sup>-1</sup>), 1.2% Ag/γ-Al<sub>2</sub>O<sub>3</sub> (141 m<sup>2</sup> g<sup>-1</sup>), and 10% Ag/γ-Al<sub>2</sub>O<sub>3</sub> (120 m<sup>2</sup> g<sup>-1</sup>). The alumina was active and selective for the formation of N<sub>2</sub> at higher temperatures, i.e., above 400°C, under these experimental conditions. It is interesting to note that some N<sub>2</sub>O and especially high concentrations of NO<sub>2</sub> were observed over the alumina after complete propene conversion, i.e., above 565°C. On the contrary, some NH<sub>3</sub> could be observed but only before complete propene conversion. The 1.2% Ag/γ-Al<sub>2</sub>O<sub>3</sub> yielded similar conversions to N<sub>2</sub> as those obtained over the alumina but at lower temperatures. Low concentrations of N<sub>2</sub>O, NO<sub>2</sub>, and NH<sub>3</sub> were also obtained in this case. The activity of the high-loaded silver catalyst was significantly different from that of the γ-Al<sub>2</sub>O<sub>3</sub> and the 1.2% Ag/γ-Al<sub>2</sub>O<sub>3</sub>. Complete combustion of the reductant was achieved at 350°C over the 10% Ag/γ-Al<sub>2</sub>O<sub>3</sub>, in contrast to the temperatures of 100% combustion of reductant over 1.2% Ag/γ-Al<sub>2</sub>O<sub>3</sub> and γ-Al<sub>2</sub>O<sub>3</sub> of 500 and 565°C, respectively. In addition, the N<sub>2</sub> yield remained significantly lower than that of N<sub>2</sub>O (obtained at the lower temperatures) and NO<sub>2</sub> (obtained at the higher temperatures). Over the 10% Ag/γ-Al<sub>2</sub>O<sub>3</sub> and at the higher temperatures, the conversion to NO<sub>2</sub> was limited by the thermodynamics of the reaction (see dotted line in Fig. 1):



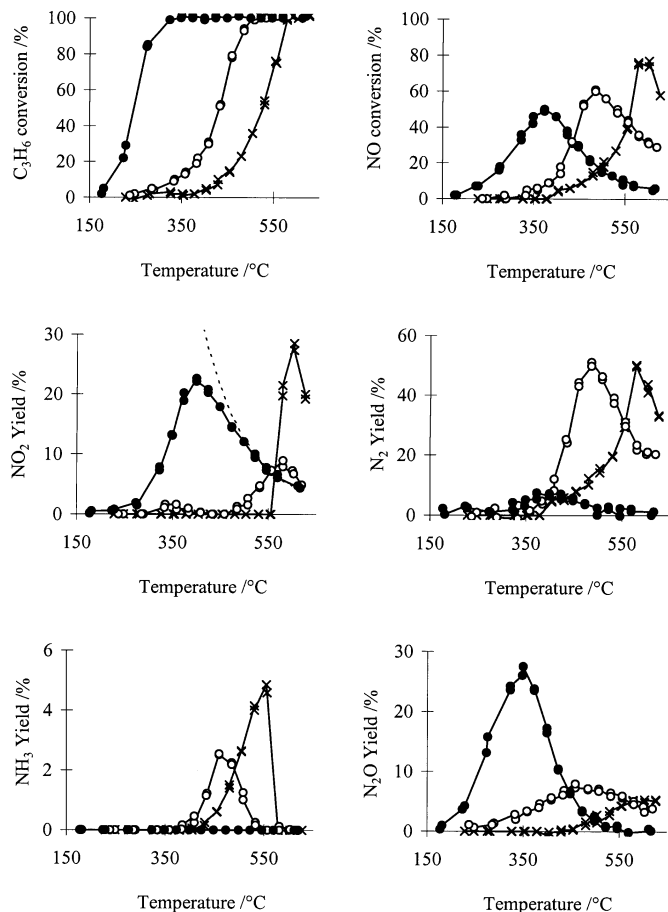


FIG. 1.  $C_3H_6$ -SCR of NO over  $\gamma-Al_2O_3$  (x), 1.2% Ag/ $\gamma-Al_2O_3$  (○) and 10% Ag/ $\gamma-Al_2O_3$  (●) catalysts as a function of temperature. Feed: 0.05% NO + 0.05%  $C_3H_6$  + 2.5%  $O_2/He$ , W/F = 0.06 g s  $cm^{-3}$  (GHSV ~ 50,000  $h^{-1}$ ). The dotted line in the plot giving the  $NO_2$  yield represents the thermodynamic limit associated to the reaction  $NO + \frac{1}{2}O_2 \rightleftharpoons NO_2$ .

One of the striking features of the catalytic data reported in Fig. 1 was the sharp increase in the  $NO_2$  yield obtained over the alumina as soon as complete conversion of propene was achieved, at ca. 565°C. The values of  $NO_2$  yield obtained at these temperatures were significantly higher than that allowed by the thermodynamics of Eq. [1]. It has to be stressed that identical plots were obtained independently of using increasing or decreasing temperature profiles and no change in the yield of  $NO_2$  was observed after several hours on stream. A  $NO_2$  yield in slight excess of the thermodynamic limit was also observed over the 1.2% Ag/ $\gamma-Al_2O_3$ , although the difference between these two values was within the experimental margin of error.

### 3.2. Effect of the W/F on the $C_3H_6$ -SCR of NO over $\gamma-Al_2O_3$ at 590°C

Conversions to  $NO_2$  in excess of the thermodynamic limits of Eq. [1] were obtained during the  $C_3H_6$ -SCR of

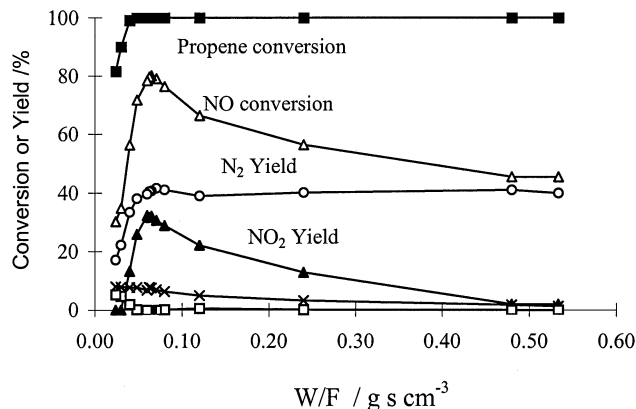


FIG. 2. Effect of the W/F on the  $C_3H_6$ -SCR of NO over  $\gamma-Al_2O_3$  at 590°C: propene conversion (■), NO conversion (△),  $N_2$  yield (○),  $NO_2$  yield (▲),  $N_2O$  yield (×) and  $NH_3$  yield (□). Feed: 0.05% NO + 0.05%  $C_3H_6$  + 2.5%  $O_2/He$ .

NO over  $\gamma-Al_2O_3$  at temperatures above 565°C, this being the temperature above which complete propene conversion was obtained (Fig. 1). Higher than expected concentrations of  $NO_2$  have also recently been reported by our laboratory for the same reaction and catalyst under conditions where 100% propene conversion was achieved by steadily increasing the W/F at a fixed temperature of 540°C (19). Figure 2 shows the results of a similar study carried out at 590°C and over a broader range of W/F values than reported previously. The results show that, at a W/F = 0.03 g s  $cm^{-3}$ , propene conversion was 90% and no  $NO_2$  could be observed while the  $N_2$  yield was 22%. At W/F = 0.06 g s  $cm^{-3}$ , propene conversion was completed and the  $NO_2$  yield reached a maximum at 32% while the  $N_2$  yield was 40%. With further increases in the W/F value, the  $N_2$  yield remained constant whereas the  $NO_2$  yield steadily decreased, the latter being converted back to NO. Figure 3 shows the experimental molar ratio  $NO_2/NO$  as a function

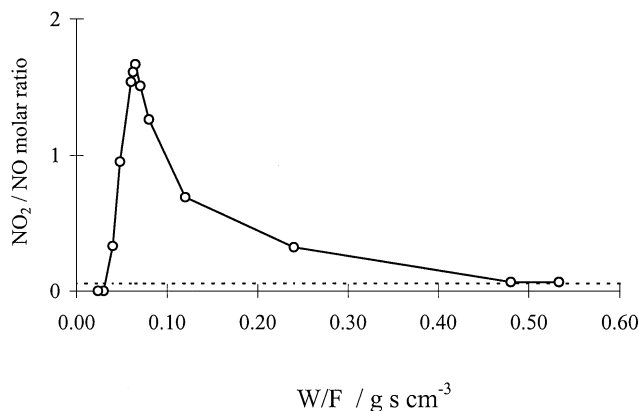


FIG. 3. Effect of the W/F on the  $C_3H_6$ -SCR of NO over  $\gamma-Al_2O_3$  at 590°C:  $NO_2/NO$  experimental ratio (○) and theoretical thermodynamic ratio (dotted line). Feed: 0.05% NO + 0.05%  $C_3H_6$  + 2.5%  $O_2/He$ .

of the W/F at 590°C, related to the data in Fig. 2. The dotted line represents the thermodynamic  $\text{NO}_2/\text{NO}$  ratio (i.e., 0.055) associated with Eq. [1] at the same temperature. Upon complete conversion of propene, the experimental ratio of  $\text{NO}_2/\text{NO}$ , on one hand, increased from zero to well beyond the thermodynamic limit, reaching a value of 1.7 at  $W/F = 0.06 \text{ g s cm}^{-3}$ . On the other hand, with further increases in the W/F, the value of the ratio decreased toward the thermodynamic figure associated with Eq. [1]. It has to be stressed that identical plots were obtained independently of using increasing or decreasing W/F values.

### 3.3. Effect of the Partial Pressure of Propene on the $\text{C}_3\text{H}_6$ -SCR of NO over $\gamma\text{-Al}_2\text{O}_3$ at 590°C

The effect of using increasing propene concentration in the reaction feed was investigated at 590°C (Fig. 4). In these experimental conditions, complete propene conversion was obtained at a feed concentration below ca. 900 ppm (propene conversion was 97.5% at 1000 ppm). Without any propene, NO was converted only to a small extent to  $\text{NO}_2$  (i.e., yield of ca. 2%). With addition of only 100 ppm of propene into the feed, more  $\text{NO}_2$  and also some reduction products, i.e.,  $\text{N}_2$  and  $\text{N}_2\text{O}$ , were observed. With 300 ppm of propene in the feed, the  $\text{NO}_2$  yield was at its maximum value. It must be stressed that below 300 ppm, the yield of  $\text{NO}_2$  was significantly higher than that of  $\text{N}_2$ . With higher propene concentrations, the  $\text{NO}_2$  yield decreased and  $\text{N}_2$  became the main product of the reaction. The  $\text{NO}_2$  concentrations obtained were higher than that expected from the Eq. [1] when using initial concentrations of propene higher than zero and not exceeding 1000 ppm. At the higher propene concentrations investigated, the  $\text{N}_2$  yield decreased, while significant proportions of  $\text{N}_2\text{O}$  and  $\text{NH}_3$  were observed.

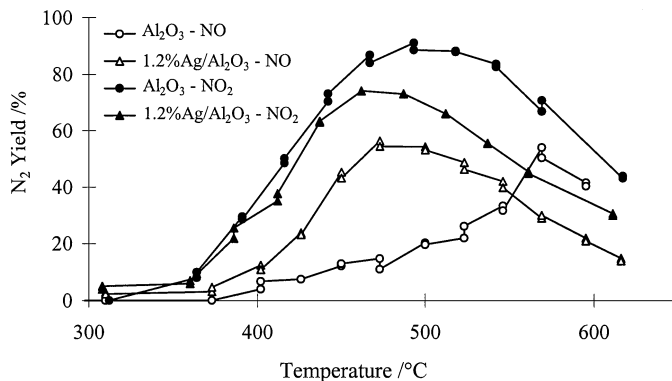


FIG. 5. Conversion to  $\text{N}_2$  during the  $\text{C}_3\text{H}_6$ -SCR of NO (open symbol) and  $\text{NO}_2$  (filled symbol) over  $\gamma\text{-Al}_2\text{O}_3$  (circle) and 1.2%  $\text{Ag}/\gamma\text{-Al}_2\text{O}_3$  (triangle) as a function of temperature. Feed: 0.05%  $\text{NO}_x + 0.05\%$   $\text{C}_3\text{H}_6 + 2.5\%$   $\text{O}_2/\text{He}$ ,  $W/F = 0.06 \text{ g s cm}^{-3}$ .

### 3.4. Comparison of the Catalytic Activity for the $\text{C}_3\text{H}_6$ -SCR of NO and $\text{NO}_2$

The  $\gamma\text{-Al}_2\text{O}_3$  and 1.2%  $\text{Ag}/\gamma\text{-Al}_2\text{O}_3$  appeared to be the most interesting catalyst with regard to the reduction of NO to  $\text{N}_2$  (Fig. 1). The beneficial effect of using  $\text{NO}_2$  instead of NO as a starting  $\text{NO}_x$  molecule has already been reported for the  $\text{C}_3\text{H}_6$ -SCR over  $\gamma\text{-Al}_2\text{O}_3$ -based catalysts (5, 11). This is exemplified in Fig. 5 which shows the  $\text{N}_2$  yield obtained over our  $\gamma\text{-Al}_2\text{O}_3$  and 1.2%  $\text{Ag}/\gamma\text{-Al}_2\text{O}_3$  using both NO and  $\text{NO}_2$ . On one hand, the most active combination of catalyst and feed was  $\gamma\text{-Al}_2\text{O}_3\text{-NO}_2$ , which gave the highest  $\text{N}_2$  yields over the broadest temperature range. On the other hand, the least active combination was  $\gamma\text{-Al}_2\text{O}_3\text{-NO}$ . Interestingly, the combinations using  $\text{NO}_2$  gave similar conversions to  $\text{N}_2$  at lower temperatures over both the  $\gamma\text{-Al}_2\text{O}_3$  and the 1.2%  $\text{Ag}/\gamma\text{-Al}_2\text{O}_3$ . Similar to the case of  $\text{Co}/\gamma\text{-Al}_2\text{O}_3$  materials (5), these results could suggest that the only role of silver (at this low loading) was to act as a promoter for the oxidation of NO to  $\text{NO}_2$ , which would be the rate-determining step of the  $\text{C}_3\text{H}_6$ -SCR reaction over the alumina.

### 3.5. Catalytic Activity for the Reaction: $\text{NO} + \frac{1}{2}\text{O}_2 \rightleftharpoons \text{NO}_2$

To assess the role of the silver in the reaction scheme, the activity of the  $\gamma\text{-Al}_2\text{O}_3$  and the 1.2%  $\text{Ag}/\gamma\text{-Al}_2\text{O}_3$  for the oxidation of NO to  $\text{NO}_2$  was measured (Fig. 6). For completeness, the data for the oxidation activity of the 10%  $\text{Ag}/\gamma\text{-Al}_2\text{O}_3$  is also shown. This sample displayed high activity for the formation of  $\text{NO}_2$  which reached the limit of yield imposed by the thermodynamics of Eq. [1] at 500°C. Interestingly, the  $\text{NO}_2$  yield obtained over the 1.2%  $\text{Ag}/\gamma\text{-Al}_2\text{O}_3$  was similar to that obtained over the alumina. Moreover, both catalysts exhibited  $\text{NO}_2$  yields significantly lower than the  $\text{N}_2$  yields observed in the corresponding SCR reaction over the whole temperature range investigated (see Fig. 1). These results apparently contradict the model suggested

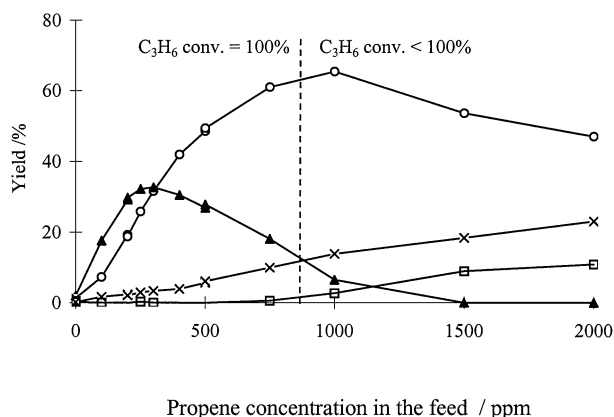


FIG. 4. Effect of the feed concentration of  $\text{C}_3\text{H}_6$  on the  $\text{C}_3\text{H}_6$ -SCR of NO over  $\gamma\text{-Al}_2\text{O}_3$  at 590°C:  $\text{N}_2$  yield ( $\circ$ ),  $\text{NO}_2$  yield ( $\blacktriangle$ ),  $\text{N}_2\text{O}$  yield ( $\times$ ) and  $\text{NH}_3$  yield ( $\square$ ). Feed: 0–0.2%  $\text{C}_3\text{H}_6 + 0.05\%$   $\text{NO} + 2.5\%$   $\text{O}_2/\text{He}$ ,  $W/F = 0.06 \text{ g s cm}^{-3}$ .

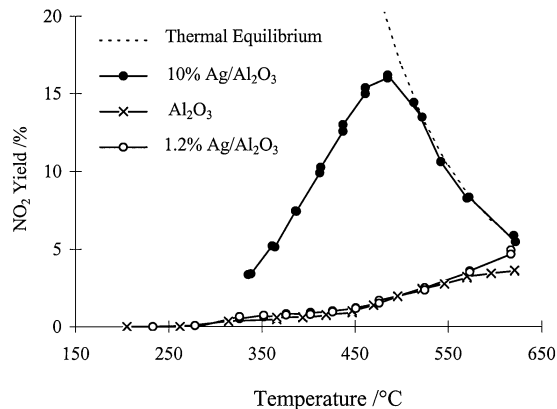


FIG. 6. Conversion of NO to NO<sub>2</sub> over  $\gamma$ -Al<sub>2</sub>O<sub>3</sub> (×), 1.2% Ag/ $\gamma$ -Al<sub>2</sub>O<sub>3</sub> (○) and 10% Ag/ $\gamma$ -Al<sub>2</sub>O<sub>3</sub> (●) catalysts as a function of temperature. Feed: 0.05% NO + 5% O<sub>2</sub> in Ar, W/F = 0.06 g s cm<sup>-3</sup>.

earlier, in which the oxidation of NO by O<sub>2</sub> to NO<sub>2</sub> was proposed to be one of the reaction steps. This step should be at least as fast as the rate-determining step of the overall SCR reaction. These apparent low activities for the forward reaction of Eq. [1] in the absence of any reductant could be explained by the poisoning of the catalysts by NO<sub>2</sub>, as was suggested in the case of Co/ $\gamma$ -Al<sub>2</sub>O<sub>3</sub> catalysts (10). Figure 7 shows the activity of the same materials for the partial decomposition of NO<sub>2</sub> to NO and  $\frac{1}{2}$ O<sub>2</sub>. The 10% Ag/ $\gamma$ -Al<sub>2</sub>O<sub>3</sub> catalyst achieved equilibrium yields at temperatures higher than 450°C, whereas the alumina and 1.2% Ag/ $\gamma$ -Al<sub>2</sub>O<sub>3</sub> exhibited much lower activities.

### 3.6. *In situ* DRIFTS and Thermogravimetric Studies of the Reaction: NO + $\frac{1}{2}$ O<sub>2</sub> ⇒ ad-NO<sub>x</sub>

The formation of adsorbed NO<sub>x</sub> (ad-NO<sub>x</sub>) species over the Al<sub>2</sub>O<sub>3</sub> and the Ag/ $\gamma$ -Al<sub>2</sub>O<sub>3</sub> materials was studied by *in situ* DRIFTS and thermogravimetric analyses at 400°C. A nitrite NO<sub>2</sub><sup>-</sup> species (1235 cm<sup>-1</sup>, Table 2) was observed on the surface of the  $\gamma$ -Al<sub>2</sub>O<sub>3</sub> only minutes after exposure

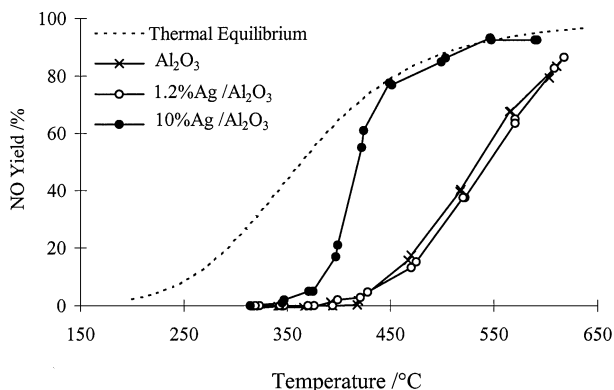


FIG. 7. Conversion of NO<sub>2</sub> to NO over  $\gamma$ -Al<sub>2</sub>O<sub>3</sub> (×), 1.2% Ag/ $\gamma$ -Al<sub>2</sub>O<sub>3</sub> (○) and 10% Ag/ $\gamma$ -Al<sub>2</sub>O<sub>3</sub> (●) catalysts as a function of temperature. Feed: 0.05% NO<sub>2</sub> + 5% O<sub>2</sub> in Ar, W/F = 0.06 g s cm<sup>-3</sup>.

TABLE 2

Bands Observed on Alumina and Ag/Alumina Material during DRIFTS Experiments and the Corresponding Surface Species and Vibrations To Which They Were Assigned (s = Symmetric, a = Asymmetric  $\nu$  = Stretching, and  $\delta$  = Bending)

Wavenumber (cm <sup>-1</sup> )	Surface species	Vibration	References
1585	Carboxylate COO <sup>-</sup>	$\nu_{\text{OCO}}^{\text{a}}$	25, 27
1460		$\nu_{\text{OCO}}^{\text{s}}$	
3005	Formate HCOO <sup>-</sup>	$\nu_{\text{OCO}}^{\text{a}} + \delta_{\text{CH}}$	25, 26, 27
2910		$\nu_{\text{CH}}$	
1595		$\nu_{\text{OCO}}^{\text{a}}$	
1390		$\delta_{\text{CH}}$	
1380		$\nu_{\text{OCO}}^{\text{s}}$	
1550		Nitrate NO <sub>3</sub> <sup>-</sup>	
1250	$\nu_{\text{ONO}}^{\text{a}}$		
1590	Nitrate NO <sub>3</sub> <sup>-</sup>	$\nu_{\text{N=O}}$	21, 22
1305		$\nu_{\text{ONO}}^{\text{a}}$	
1235	Nitrite NO <sub>2</sub> <sup>-</sup>	$\nu_{\text{ONO}}^{\text{a}}$	21
1560	Ad-NO <sub>x</sub>		23, 24
1300	bulk-like NO <sub>2</sub> <sup>-</sup> ?		
1645	Organo-nitrite or oxime?	$\nu_{\text{N=O}}$ or $\nu_{\text{N=O}}$	14, 31
1380	Organo-nitro?	$\nu_{\text{ONO}}^{\text{a}}$	24
2230	Isocyanate -NCO		29
2135	Cyanide -CN		30

to the NO/O<sub>2</sub> mixture, with the intensity of the absorption band remaining unchanged after 3 h on stream (Fig. 8a). After several hours of reaction, the formation of nitrate NO<sub>3</sub><sup>-</sup> species (1550 cm<sup>-1</sup>, (21, 22)) was also observed. The *in situ* DRIFTS analysis over the 1.2% Ag/ $\gamma$ -Al<sub>2</sub>O<sub>3</sub> revealed that nitrate species were formed only minutes after exposure to a NO/O<sub>2</sub> stream and that the intensity of their absorption bands continued to grow gradually with time on stream (Fig. 8b). Two types of bidentate nitrates were formed, one species with bands at 1550 and 1255 cm<sup>-1</sup> and another one with bands at 1590 (shoulder) and 1305 cm<sup>-1</sup>. Figure 8c shows the *in situ* DRIFTS spectra obtained over 10% Ag/ $\gamma$ -Al<sub>2</sub>O<sub>3</sub>. Several ad-NO<sub>x</sub> species were formed within minutes of the introduction of the NO/O<sub>2</sub> stream; the bands around 1560 cm<sup>-1</sup> are probably similar to the bidentate nitrates observed over the materials discussed above. The intensity of the band at 1300 cm<sup>-1</sup> was higher than that expected for the band associated with the bidentate nitrate at 1590 cm<sup>-1</sup>. As a result, this band at 1300 cm<sup>-1</sup> can probably be attributed to bulk-like nitrite species (23, 24). Figure 9 reports the relative weight uptake obtained for the same catalysts under the same experimental conditions. The weight uptake was significantly faster with the 1.2% Ag/ $\gamma$ -Al<sub>2</sub>O<sub>3</sub> than it was with the alumina. This set of data shows that both the alumina and the 1.2% Ag/ $\gamma$ -Al<sub>2</sub>O<sub>3</sub> were able to oxidise NO to ad-NO<sub>x</sub> species and that the latter was significantly more active for the adsorption than the former. The similarly low

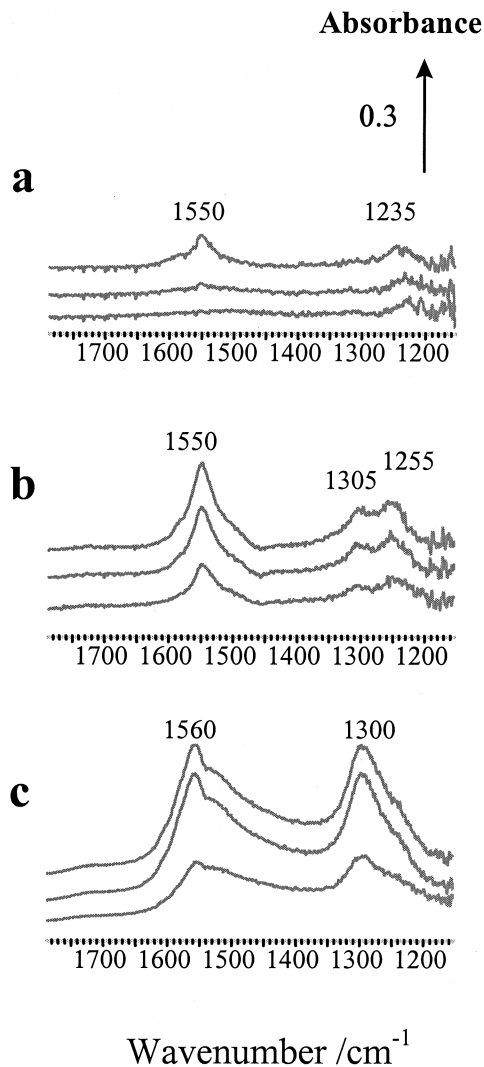


FIG. 8. *In situ* DRIFTS analysis of the formation of ad-NO<sub>x</sub> species at 400°C over (a)  $\gamma$ -Al<sub>2</sub>O<sub>3</sub>, (b) 1.2% Ag/ $\gamma$ -Al<sub>2</sub>O<sub>3</sub>, and (c) 10% Ag/ $\gamma$ -Al<sub>2</sub>O<sub>3</sub>. For each catalyst, time on stream was 15 min (lower spectrum), 60 min (middle spectrum), and 180 min (upper spectrum). Feed: 0.05% NO + 2.5% O<sub>2</sub>/He.

activity of these two samples for the oxidation of NO to NO<sub>2</sub> reported in the previous section suggested that the ad-NO<sub>x</sub> species formed on the 1.2% Ag/ $\gamma$ -Al<sub>2</sub>O<sub>3</sub> were stable and, once formed on the surface of the catalyst, could not readily be desorbed as NO<sub>2</sub>. Therefore, it appears likely that the surface of the 1.2% Ag/ $\gamma$ -Al<sub>2</sub>O<sub>3</sub> catalyst can be poisoned by strongly bound nitrates which form in the presence of NO/O<sub>2</sub>. The low steady-state NO<sub>2</sub> formation observed in Fig. 6 could, hence, mostly be attributed to the alumina, which was also probably poisoned to some extent by the ad-NO<sub>x</sub> species.

### 3.7. *In situ* DRIFTS of the C<sub>3</sub>H<sub>6</sub>-SCR of NO

For the experiments reported in this section the reaction temperature was increased from 100 to 600°C in intervals of

100°C. The spectra obtained after 40-min dwelling at a given temperature are shown. Unlike the case of the catalytic data for which steady-state measurements were usually obtained within minutes of a change in the experimental conditions, it was observed in other experiments (not shown) that the achievement of steady-state *in situ* DRIFTS spectra could require significantly longer periods. This was due to slower achievement of equilibrium surface coverage of “spectator” species associated with slower side reactions. Therefore, the data reported here should be regarded as bearing in them a character of temperature time-programmed analysis. In addition, the W/F during the catalytic and DRIFTS experiments were different, typically  $60 \times 10^{-3} \text{ g s cm}^{-3}$  in the former case and approximately  $18 \times 10^{-3} \text{ g s cm}^{-3}$  in the latter. Therefore, the DRIFTS experiments provided essentially a qualitative description of the nature and reactivity of the species observed at the catalyst surface at a given temperature.

Figure 10 shows the *in situ* DRIFTS spectra obtained during the title reaction over  $\gamma$ -Al<sub>2</sub>O<sub>3</sub>. The spectra at all temperatures were relatively simple and were essentially composed of the bands associated with a formate species (i.e., bands at 3005, 2910, 1595, 1390, and 1380 cm<sup>-1</sup>) and a carboxylate species with bands at 1585 and 1460 cm<sup>-1</sup> (25–27) (Table 2). Whereas the carboxylate observed at the higher temperatures is most likely a free carboxylate species (precursor of CO<sub>2</sub>), the carboxylate group observed at the lower temperatures could also be that of an acetate species (28). At 300°C, a nitrite species (1235 cm<sup>-1</sup> (21)) was readily formed upon admission of the reaction stream over the sample but was gradually displaced with time on stream.

Figure 11 shows the *in situ* DRIFTS spectra obtained during the same reaction over the 1.2% Ag/ $\gamma$ -Al<sub>2</sub>O<sub>3</sub>. In

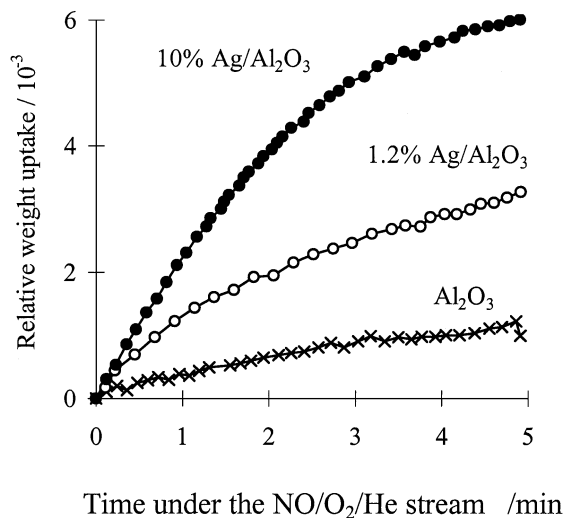


FIG. 9. Thermogravimetric analysis of the formation of ad-NO<sub>x</sub> species at 400°C over  $\gamma$ -Al<sub>2</sub>O<sub>3</sub> (×), 1.2% Ag/ $\gamma$ -Al<sub>2</sub>O<sub>3</sub> (○), and 10% Ag/ $\gamma$ -Al<sub>2</sub>O<sub>3</sub> (●) as a function of time: Feed: 0.05% NO + 2.5% O<sub>2</sub>/He.

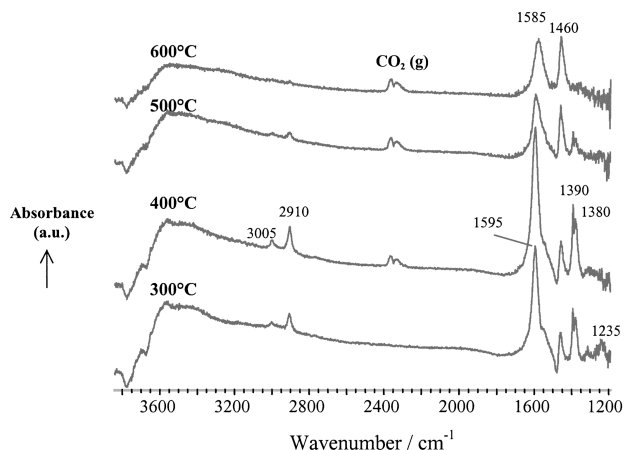


FIG. 10. *In situ* DRIFTS of  $\gamma$ -Al<sub>2</sub>O<sub>3</sub> during the C<sub>3</sub>H<sub>6</sub>-SCR of NO. Feed: 0.05% NO + 0.05% C<sub>3</sub>H<sub>6</sub> + 2.5% O<sub>2</sub>/He.

this case, essentially no formate species were present at any temperature but instead mainly nitrites (bands at 1235 and 1320 cm<sup>-1</sup>) and nitrates species (bands at 1255, 1300, and 1545 cm<sup>-1</sup>) were observed (Table 2, (21)). At 300°C, absorption bands assigned to isocyanate (2230 cm<sup>-1</sup>, (29)) and cyanide (2135 cm<sup>-1</sup>, (30)) species were also observed. At 400°C, the isocyanate band disappeared, whereas a band at 1460 cm<sup>-1</sup> appeared, indicating the presence of surface carboxylate groups (the other associated band at 1585 cm<sup>-1</sup> being masked by that of the nitrates species). A minor band at 1380 cm<sup>-1</sup> was also observed. At this temperature, some gas-phase CO<sub>2</sub> could be observed, which indicated that significant propene conversion was attained. The coincidence of the disappearance of the isocyanate band at the temperature at which the N<sub>2</sub> yield started to be significant (see Figs. 1 and 5) suggested that the isocyanate could be an intermediate of the SCR reaction, as already proposed by other authors for the same system (14). Eventually, the cyanide species was also displaced but with longer dwelling times at 400°C. At 500°C, a band at 1645 cm<sup>-1</sup> was observed,

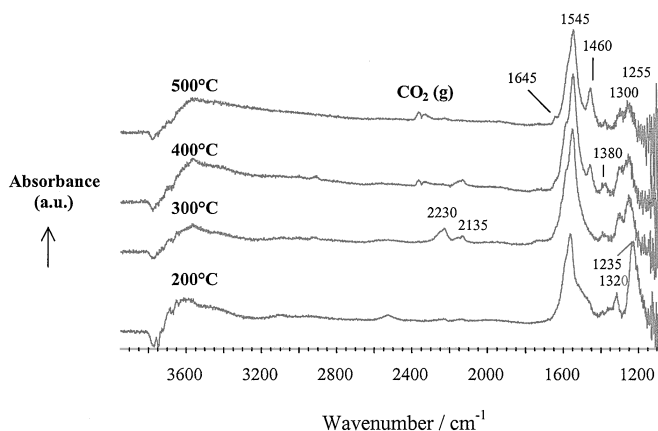


FIG. 11. *In situ* DRIFTS of 1.2% Ag/ $\gamma$ -Al<sub>2</sub>O<sub>3</sub> during the C<sub>3</sub>H<sub>6</sub>-SCR of NO. Feed: 0.05% NO + 0.05% C<sub>3</sub>H<sub>6</sub> + 2.5% O<sub>2</sub>/He.

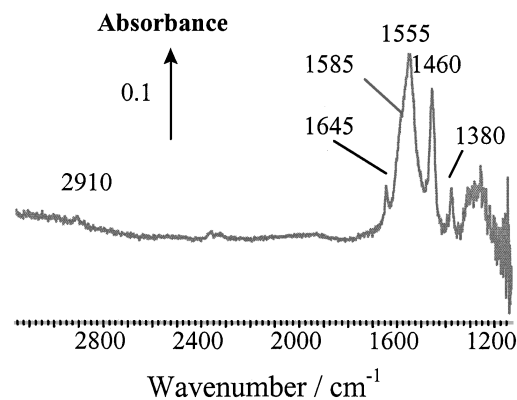


FIG. 12. *In situ* DRIFTS of 1.2% Ag/ $\gamma$ -Al<sub>2</sub>O<sub>3</sub> during the C<sub>3</sub>H<sub>6</sub>-SCR of NO at 400°C. The sample was brought to 400°C in Ar and then exposed to the stream of reaction; the spectra were recorded after 2 h. Feed: 0.05% NO + 0.05% C<sub>3</sub>H<sub>6</sub> + 2.5% O<sub>2</sub>/He.

which was probably masked at lower temperatures by the nitrates bands. In an experiment made on an isothermal dwelling at 400°C and over longer durations (Fig. 12), the band at 1645 cm<sup>-1</sup> was more clearly resolved and appeared to be formed parallel to the band at 1380 cm<sup>-1</sup>. The absorption peak centred at 1645 cm<sup>-1</sup> could correspond to that of organo-nitrite compound (14, 31) or oxime species (6) and that at 1380 cm<sup>-1</sup> to organo-nitro compounds (24).

Figure 13 shows the *in situ* DRIFTS spectra obtained over the 10% Ag/ $\gamma$ -Al<sub>2</sub>O<sub>3</sub>. At 200°C, the surface, on one hand, was covered by carboxylates species (ca. 1595 and 1455 cm<sup>-1</sup>) and other compounds which were not readily determinable. On the other hand, at the higher temperatures, only ad-NO<sub>x</sub> species were observed, similar to those obtained under a NO/O<sub>2</sub> stream (see Fig. 8c).

### 3.8. *In Situ* DRIFTS of the C<sub>3</sub>H<sub>6</sub>-SCR of NO<sub>2</sub>

The C<sub>3</sub>H<sub>6</sub>-SCR of NO<sub>2</sub> over  $\gamma$ -Al<sub>2</sub>O<sub>3</sub> was also investigated (Fig. 14). At 300°C, the *in situ* DRIFTS analysis

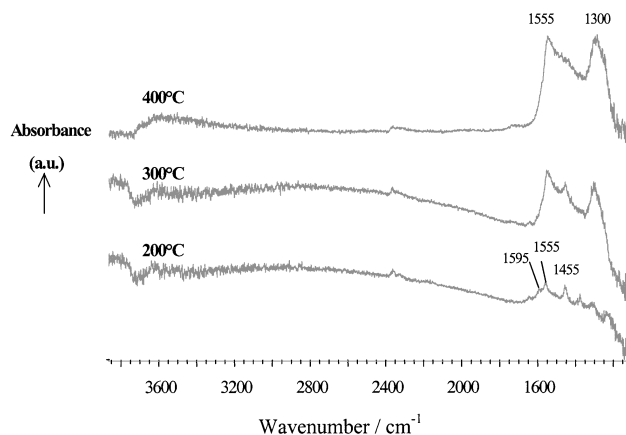


FIG. 13. *In situ* DRIFTS of 10% Ag/ $\gamma$ -Al<sub>2</sub>O<sub>3</sub> during the C<sub>3</sub>H<sub>6</sub>-SCR of NO. Feed: 0.05% NO + 0.05% C<sub>3</sub>H<sub>6</sub> + 2.5% O<sub>2</sub>/He.



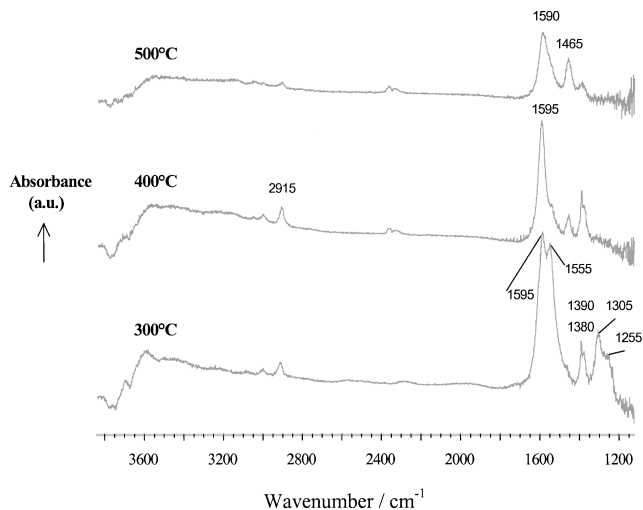


FIG. 14. *In situ* DRIFTS of  $\gamma$ - $\text{Al}_2\text{O}_3$  during the  $\text{C}_3\text{H}_6$ -SCR of  $\text{NO}_2$ . Feed: 0.05%  $\text{NO}_2$  + 0.05%  $\text{C}_3\text{H}_6$  + 2.5%  $\text{O}_2/\text{He}$ .

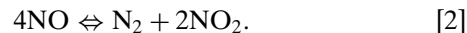
indicated the presence of both formate (i.e., bands at 3005, 2910, 1595, 1390, and 1380  $\text{cm}^{-1}$ ) and nitrate (1555, 1305, and 1255  $\text{cm}^{-1}$ ) species at the surface of the catalyst. At 400°C, only the formate species remained, along with the carboxylate group (1585 and 1465  $\text{cm}^{-1}$ ) and gas-phase  $\text{CO}_2$ . This observation should be related to the fact that the rate of  $\text{N}_2$  formation was essentially nil at 300°C, whereas the reduction proceeded to a significant extent at 400°C (Fig. 5). Hence, the nitrates species observed at 300°C were not reactive at this temperature. A similar spectrum to that at 400°C was obtained at 500°C, with an increased intensity of the bands associated with the carboxylate and a decreased intensity of the bands associated with the formates. The fact that no ad- $\text{NO}_x$  species could be detected on the surface of the alumina above 300°C was rather surprising and suggests that the  $\text{NO}_2$  may be readily reacting with an adsorbed species to yield  $\text{N}_2$ .

#### 4. DISCUSSION

##### 4.1. Origin of $\text{NO}_2$ during the $\text{C}_3\text{H}_6$ -SCR of NO over Alumina

High surface area  $\gamma$ - $\text{Al}_2\text{O}_3$  is one of the most active single oxides for the formation of  $\text{N}_2$  during the SCR of NO with light hydrocarbons such as ethene, propene, and propane, although it is only active at temperatures typically above 400°C. A widely accepted model for the reaction mechanism suggests that the initial step is the  $\text{O}_2$  oxidation of NO to  $\text{NO}_2$ , which is followed by the reduction of  $\text{NO}_2$  with the hydrocarbon. However, the data reported here (Figs. 1 and 3) and earlier published works show that yields of  $\text{NO}_2$  in excess of the thermodynamic limit associated with Eq. [1] could be obtained during the  $\text{C}_3\text{H}_6$ -SCR of NO. This observation rules out Eq. [1] as the main route for the for-

mation of  $\text{NO}_2$ . On the basis of thermodynamic calculations and reports from the literature, two alternative routes could be proposed. One of them is based on a disproportionation reaction (32):



The stoichiometry of Eq. [2] implies that the  $\text{N}_2$  and  $\text{NO}_2$  yields (based on nitrogen) should be equal. In fact, as  $\text{NO}_2$  could further readily react with the propene to give  $\text{N}_2$ , the expected  $\text{NO}_2$  yield should be lower than that of  $\text{N}_2$ . However,  $\text{NO}_2$  yields significantly higher than that of  $\text{N}_2$  could be obtained when using low concentrations of reductant in the feed (Fig. 4), thus discarding Eq. [2] as the major route for  $\text{NO}_2$  formation. A second possibility for  $\text{NO}_2$  formation involves the selective oxidation of the reductant by both NO and  $\text{O}_2$  to form an organo-nitro or -nitrite compound (Eq. [3a]). Organo-nitro and -nitrite species have often been quoted as possible intermediates of SCR reactions (31, 33–35). The combustion of this molecule by  $\text{O}_2$  would lead to  $\text{NO}_2$  (Eq. [3b]):



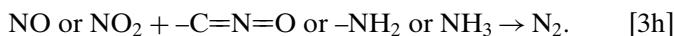
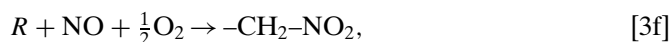
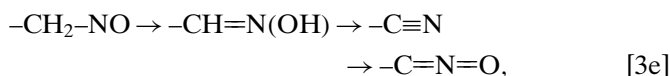
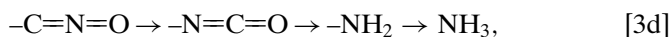
In earlier work (19), nitro-methane was used as an example for the organo- $\text{NO}_x$  compound. Thermodynamic data for this molecule is available at high temperatures; as a result, the free enthalpy of reactions with this molecule can be calculated. Thus, whether the thermodynamics will allow reactions [3a] and [3b] to proceed under the conditions of interest and the possible relevance of this reaction scheme for the formation of high concentrations of  $\text{NO}_2$  can be ascertained. However, if such a route applies to a major extent during the  $\text{C}_3\text{H}_6$ -SCR of NO over  $\gamma$ - $\text{Al}_2\text{O}_3$ , it is likely that the intermediate compound could correspond to some other organo-nitro or -nitrite compounds and possibly to a species which is only present in an adsorbed state. Obuchi *et al.* reported the presence of carbonaceous radical species over the surface of alumina during the  $\text{C}_3\text{H}_6$ -SCR of NO (36). The reactivity of such compounds should be high toward  $\text{O}_2$  (paramagnetic) and especially NO which is a free radical. Otsuka *et al.* provided further support for the relevance of organo-nitrogen species to de- $\text{NO}_x$  chemistry (37). These authors found that nitro-alkane compounds were formed during the gas-phase oxidation of light alkanes in the presence of NO. Although alkyl-nitrite could not be directly observed, these authors suggested that nitrite species were important intermediates in the reaction scheme involved. Interestingly, Smith *et al.* (38) reported the homogeneous formation of the concentration of  $\text{NO}_2$  in excess of the limits determined by Eq. [1] from mixtures containing NO,  $\text{O}_2$ , and hydrocarbon species at temperatures above 500°C. These authors invoked the occurrence of free radical reactions including  $\text{HO}_2$  and alkyl radicals which would thermodynamically justify the

high proportion of NO<sub>2</sub> observed. The space velocities used by these authors (up to 4,000 h<sup>-1</sup>) were, however, significantly lower than that used in the present work (typically 50,000 h<sup>-1</sup>). Although the NO conversions measured in an empty reactor were not significant in our case, the occurrence of gas-phase reactions possibly triggered by the alumina surface can nevertheless not be excluded.

Other results obtained over alumina showed that the compound from which the NO<sub>2</sub> originated was more likely to be an organo-nitrite species rather than an organo-nitro species (39). We have looked for such species by *in situ* DRIFTS measurements over the alumina, both in steady state, and transient analyses at the high temperatures typical of C<sub>3</sub>H<sub>6</sub>-SCR reactions, but no such species could yet be detected. An explanation for this could be that their concentration and lifetime is very small. This is supported by the findings of Yamaguchi (34) who reported that, for instance, nitro-methane was readily decomposed over alumina at temperatures lower than 200°C. Another possibility would be that these species are mostly short-lived gas-phase compounds.

#### 4.2. Mechanistic Considerations of the C<sub>3</sub>H<sub>6</sub>-SCR of NO over Alumina

For the rest of the discussion, we shall assume, on one hand, the relevance of Eqs. [3a] and [3b] to the reaction mechanism of the C<sub>3</sub>H<sub>6</sub>-SCR of NO over alumina with regard to the formation of NO<sub>2</sub>. On the other hand, this system needs to be completed by another set of equations to take into account the formation of NH<sub>3</sub>. This molecule was observed in significant proportions during the C<sub>3</sub>H<sub>6</sub>-SCR of NO, but only when the conversion of propene was incomplete (Figs. 1, 2, and 4). NH<sub>3</sub> can be obtained from reaction of nitromethane over alumina (34, 41), probably through the tautomerisation to the corresponding oxime followed by dehydration to a nitrile *N*-oxide (Eq. [3c]) which isomerises to an isocyanate before yielding a primary amine and NH<sub>3</sub> by hydrolysis (Eq. [3d]), as suggested over zeolitic materials (40, 41). Over alumina, the possibility of forming NH<sub>3</sub> from reaction of organo-nitrile *N*-oxides species was confirmed by Obuchi *et al.* (42). The same authors proposed that the organo-nitrile *N*-oxide were formed from organo-nitroso compounds, via enol and cyanide formation (Eq. [3e]). Therefore, the formation of organo-nitro (Eq. [3f]) and organo-nitroso (Eq. [3g]) compounds appears to be relevant to the mechanism of the C<sub>3</sub>H<sub>6</sub>-SCR of NO over alumina:



The species *R* and *R'* quoted in Eqs. [3f] and [3g] derive from propene and could be oxygenated compounds, or possibly radicals as suggested by Obuchi *et al.* (36). The *in situ* DRIFTS analysis during the SCR reaction over the alumina only revealed formate and carboxylate species (Fig. 10), similar to those observed during the simple combustion of propene by O<sub>2</sub> (not shown). The absence of any band assignable to organo-NO<sub>x</sub> compounds suggests that the concentration of these species were too low to be observed.

Many of the potential products of reaction of organo-nitrite and organo-nitro/nitroso compounds could further react to yield N<sub>2</sub>; these possibilities are gathered in Eq. [3h]. NH<sub>3</sub> is a well-known reductant of NO and NO<sub>2</sub> in O<sub>2</sub>-rich conditions over many catalytic materials (43). The intermediacy of NH<sub>3</sub> in the hydrocarbon-SCR reaction has been suggested over zeolitic catalysts (44, 45). Figures 1, 2, and 4 show that NO<sub>2</sub> was essentially observed only when NH<sub>3</sub> was not present and vice versa. This fact strongly supports the idea that a significant proportion of the N<sub>2</sub> formed arose from the reaction between NO<sub>2</sub> and NH<sub>3</sub>, or at least from the corresponding adsorbed species from which these molecules were formed. In addition, a parallel route for N<sub>2</sub> formation could also involve the reaction of NO with an adsorbed isocyanate species (i.e., -NCO + NO → N<sub>2</sub> + CO<sub>2</sub>), similar to the one proposed to be involved in CO/NO reaction over Rh catalysts (27). Over silver-alumina catalysts, isocyanate species were even shown to react to form N<sub>2</sub> more readily with NO + O<sub>2</sub> than with a O<sub>2</sub>-free NO stream (14). More work is needed to clarify which of these steps are possible over the alumina and ultimately if any of those is actually occurring during the C<sub>3</sub>H<sub>6</sub>-SCR of NO. A simplified scheme summarising the different reaction steps proposed is given in Fig. 15.

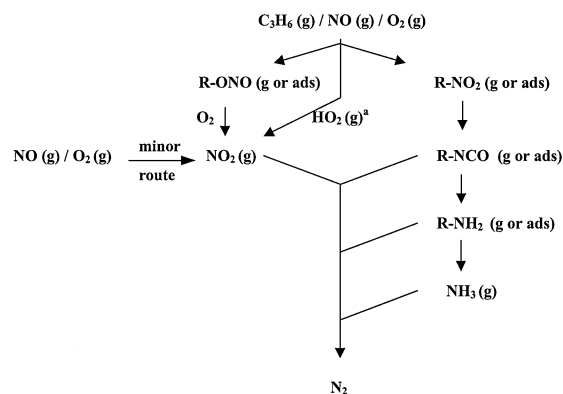


FIG. 15. Simplified reaction scheme of the C<sub>3</sub>H<sub>6</sub>-SCR of NO over  $\gamma$ -Al<sub>2</sub>O<sub>3</sub> giving the nature of the different species likely to be involved. <sup>a</sup> See Ref. (38).

#### 4.3. Utilisation of $\text{NO}_2$ for the $\text{C}_3\text{H}_6$ -SCR of $\text{NO}_x$ over Alumina

Surprisingly, the *in situ* DRIFTS spectra of the  $\text{C}_3\text{H}_6$ -SCR of NO and  $\text{NO}_2$  were similar at 400 and 500°C, temperatures at which  $\text{N}_2$  was being formed in both cases (see Figs. 5, 10, and 14). The absence of nitrate species on the alumina surface at temperatures above 300°C when using  $\text{NO}_2$  as a feed indicates that this molecule reacted from the gas phase or was decomposed immediately upon adsorption. Different roles for  $\text{NO}_2$  could be envisaged in the reaction mechanism.  $\text{NO}_2$  could provide the oxygen necessary for the activation of the reductant and thus be reduced to NO; the latter molecule was indeed observed under these conditions. The activated reductant would then react with  $\text{NO}_x/\text{O}_2$  to form the organo- $\text{NO}_x$  compounds. The formation of oxygenated molecules from propene can be obtained over oxide catalysts pretreated with  $\text{NO}_2$  (46). However, alumina displayed a poor ability for the selective oxidation of propene, in contrast to titania, for instance. Although not directly related to the SCR reaction, this observation effectively rules out the role of  $\text{NO}_2$  as an activator of the propene to a specific  $\text{C}_x\text{H}_y\text{O}_z$  intermediate. A more straightforward possibility would be that the  $\text{NO}_2$  could react with the reductant or a derived species ( $\text{C}_x\text{H}_y$  or  $\text{C}_x\text{H}_y\text{O}_z$  formed with  $\text{O}_2$ ) to directly form the organo- $\text{NO}_x$  species associated with the reaction scheme described above. The formation of alkyl-nitrite compounds from light alkanes and  $\text{NO}_2$  was suggested as being a crucial step in homogeneous selective oxidation reactions, at temperatures as low as 450°C (37). Therefore, the formation of an organo- $\text{NO}_x$  compound from propene and  $\text{NO}_2$  is imaginable under our experimental conditions. Interestingly, no ammonia was observed during the  $\text{C}_3\text{H}_6$ -SCR of  $\text{NO}_2$ . This suggests that the formation of the organo-nitro/nitroso compounds from which ammonia derives would be the rate-limiting step of the reaction when using  $\text{NO}_2$  as the reactant in place of NO.

#### 4.4. Mechanistic Considerations of the $\text{C}_3\text{H}_6$ -SCR of NO over 10% $\text{Ag}/\gamma\text{-Al}_2\text{O}_3$

The results reported here regarding the effect of the loading of silver over the alumina are consistent with the findings of Bethke *et al.* (11). These authors suggested that the difference in catalytic activity for the  $\text{C}_3\text{H}_6$ -SCR of NO between a 6 and a 2 wt%  $\text{Ag}/\gamma\text{-Al}_2\text{O}_3$  was due to the different dispersions and oxidation states of the silver on the alumina, the surface area of the latter being in the range 200–250  $\text{m}^2\text{g}^{-1}$ . The high activities for propene combustion and  $\text{N}_2\text{O}$  and  $\text{NO}_2$  formation (in the absence of propene) which were observed on our 10%  $\text{Ag}/\gamma\text{-Al}_2\text{O}_3$  can therefore be most likely attributed to the metallic character of large silver particles on the alumina. For nonsupported silver materials and under our conditions of  $\text{O}_2$  partial pressure, the metallic state of silver is thermodynamically favoured as opposed

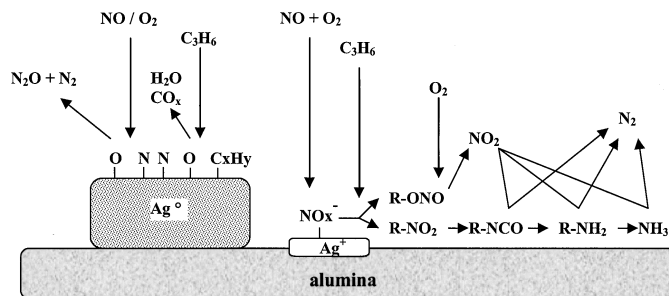


FIG. 16. The different roles of Ag during the  $\text{C}_3\text{H}_6$ -SCR over  $\text{Ag}/\gamma\text{-Al}_2\text{O}_3$ : large  $\text{Ag}^0$  particles catalyse the decomposition-reduction of NO whereas  $\text{Ag}^+$  species favours the oxidation of NO to ad- $\text{NO}_x$  species which subsequently react through the intermediacy of organonitrogen compounds.

to  $\text{Ag}_2\text{O}$  at temperatures higher than 130°C. Interestingly, the 10%  $\text{Ag}/\gamma\text{-Al}_2\text{O}_3$  material was significantly more active for the formation of  $\text{NO}_2$  during the SCR reaction (when propene conversion was completed) than during the simple  $\text{O}_2$  oxidation of NO (see Figs. 1 and 3). A sample previously used for the SCR reaction or one prerduced in  $\text{H}_2$  at 400°C gave higher activities for the  $\text{O}_2$  oxidation of NO than a calcined sample (not shown). As no deactivation nor any hysteresis were observed after use in strongly oxidative atmospheres, it is thought that the reduction (*in situ* with propene or *ex situ* with  $\text{H}_2$ ) irreversibly modified the dispersion of the metal over the alumina. The 10%  $\text{Ag}/\gamma\text{-Al}_2\text{O}_3$  catalyst displayed a catalytic behaviour somewhat similar to that of Pt-based formulations (47). The related mechanism of reaction involves the decomposition of NO into elemental nitrogen and oxygen species over a surface which is kept reduced by the reductant (3) (Fig. 16). In spite of significant activity for NO reduction at low temperatures, the high selectivity to  $\text{N}_2\text{O}$  observed on the 10%  $\text{Ag}/\gamma\text{-Al}_2\text{O}_3$  catalyst makes this type of material of rather limited interest for the  $\text{C}_3\text{H}_6$ -SCR of NO.

#### 4.5. Mechanistic Considerations on the $\text{C}_3\text{H}_6$ -SCR of NO over 1.2% $\text{Ag}/\gamma\text{-Al}_2\text{O}_3$

At the lower loading of 1.2%  $\text{Ag}/\gamma\text{-Al}_2\text{O}_3$  the silver was probably kept in an oxidised state, even at the higher temperatures under reaction conditions, this being due to a strong interaction with the support (11). The possibility of forming a silver aluminate was reported when using high temperature of calcination (i.e., 800°C) in a steam-containing atmosphere (17). The activity of the 1.2%  $\text{Ag}/\gamma\text{-Al}_2\text{O}_3$  was slightly modified by prerduction with  $\text{H}_2$  at 400°C; the activity for the  $\text{O}_2$  oxidation of NO was increased by ca. 50% and the activity for the SCR activity was decreased, probably due to an increase in the direct combustion of propene. The modification upon  $\text{H}_2$  reduction could be assigned to a decrease of the dispersion of the silver. Regardless of the exact state of the silver over the (calcined)

1.2% Ag/ $\gamma$ -Al<sub>2</sub>O<sub>3</sub> during the SCR reaction, the associated catalytic properties were significantly different from that of the 10% loading sample. At 300°C, the rate for propene conversion of the former was ca. 200-fold lower than that of the latter. The 1.2% Ag/ $\gamma$ -Al<sub>2</sub>O<sub>3</sub> sample appeared to have catalytic properties for the C<sub>3</sub>H<sub>6</sub>-SCR of NO somewhat similar to those of the  $\gamma$ -Al<sub>2</sub>O<sub>3</sub> but shifted toward lower temperatures (Fig. 1). However, contrary to the case of the alumina, the NO<sub>2</sub> yield over the 1.2% Ag/ $\gamma$ -Al<sub>2</sub>O<sub>3</sub> was never in significant excess of the limit set by Eq. [1] when complete propene conversion was achieved, either by varying the temperature (Fig. 1) or the W/F at 590°C (not shown). Although both samples had identical activities for O<sub>2</sub> oxidation of NO to NO<sub>2</sub> (Fig. 6), the silver-promoted material displayed greater activity for the formation of surface nitrates (Figs. 8 and 9). This observation suggests that the role of the silver phase was to oxidise NO to inorganic ad-NO<sub>x</sub> species during the SCR reaction. This is supported by the *in situ* DRIFTS results which showed the predominant presence of nitrate species on the surface of the silver-promoted catalyst during the SCR reaction (Fig. 11), in contrast to the alumina which was covered with formate species (Fig. 10). It is likely that these nitrates would be too strongly bound to the surface to desorb and would, eventually, if no reductant was available, poison the catalyst. Hence, the low activities measured for Eq. [1] were very similar to those of the alumina. A similar explanation for the low activity of Co/ $\gamma$ -Al<sub>2</sub>O<sub>3</sub> for the oxidation of NO to NO<sub>2</sub> was proposed by Yan *et al.* (10).

The C<sub>3</sub>H<sub>6</sub>-SCR of NO<sub>2</sub> gave similar N<sub>2</sub> yields over the  $\gamma$ -Al<sub>2</sub>O<sub>3</sub> and the 1.2% Ag/ $\gamma$ -Al<sub>2</sub>O<sub>3</sub> over a broad range of temperatures (Fig. 5). This suggests that the reduction ability could essentially be attributed solely to the alumina. (The lower N<sub>2</sub> yield observed over the silver-promoted material at the higher temperatures was probably due to a higher rate of propene combustion over this sample compared to that of the alumina, the combustion reaction competing with the SCR reaction for the reducing agent.) Similar to the reaction scheme proposed for the alumina, the nitrates formed over the silver phase could be reacting with the reductant or a derived species to form organo-NO<sub>x</sub> species which would then react to yield N<sub>2</sub>. The isocyanate and cyanide species observed over the silver-promoted material could be formed from the species with the IR band at 1645 and 1380 cm<sup>-1</sup> (Figs. 11 and 12), probably organo-nitro- or -oxime species. Interestingly, the isocyanate band, on one hand, disappeared readily when the temperature was increased from 300 to 400°C, coinciding with the light-off of the SCR reaction. On the other hand, the cyanide band was more stable. This suggests that the isocyanate species would be the most reactive reaction intermediate. The promoting effect of silver on the formation of the organo-NO<sub>x</sub> species would increase their surface concentration to a noticeable extent when compared to the alu-

mina. These assumptions are supported by the findings of Sumiya *et al.* who observed the formation of an IR band at 1655 cm<sup>-1</sup> assigned to an organo-NO<sub>x</sub> species over a 5% Ag/Al<sub>2</sub>O<sub>3</sub> material under a NO/O<sub>2</sub>/C<sub>3</sub>H<sub>6</sub> flow at room temperature (14). During a temperature-programmed reaction, this compound was converted to isocyanate species, both on the silver (2230 cm<sup>-1</sup>) and the alumina (2260 cm<sup>-1</sup>). These authors reported that the isocyanate species were reacting with NO, O<sub>2</sub>, and especially with NO/O<sub>2</sub> to yield N<sub>2</sub>. However, no clear conclusions could be drawn as to which of the Al-NCO or Ag-NCO was reacting faster. Following our results and those of the literature, a simplified model of the mechanism of the C<sub>3</sub>H<sub>6</sub>-SCR of NO over the 1.2% Ag/ $\gamma$ -Al<sub>2</sub>O<sub>3</sub> material can be obtained by adding the set of equations [4a]–[4d] to those already described for the alumina (Eqs. [3a]–[h]) (Fig. 16):



Hence, the promoting effect of the silver that we would like to propose over the 1.2% Ag/ $\gamma$ -Al<sub>2</sub>O<sub>3</sub> is characterised by increased rates of formation of organo-NO<sub>x</sub> compounds (Eqs. [4b]–[4d]) as compared to the case of the  $\gamma$ -Al<sub>2</sub>O<sub>3</sub> (Eqs. [3a], [3f], and [3g]). However, it is not clear yet if the decomposition/reactions of these organo-NO<sub>x</sub> species occur on both the silver and the alumina phases or predominantly on one of those. The precise nature of the reacting species derived from propene still needs to be determined.

## 5. CONCLUSIONS

The formation of NO<sub>2</sub> during the C<sub>3</sub>H<sub>6</sub>-SCR of NO over  $\gamma$ -Al<sub>2</sub>O<sub>3</sub> is not achieved through the oxidation of NO with O<sub>2</sub>. A mechanism (possibly partly homogeneous) involving the formation of organo-nitrite species followed by their decomposition/oxidation is suggested to be the route accounting for the formation of NO<sub>2</sub>. The promoting role of low loadings of silver (i.e., 1.2 wt%, probably in an oxidised state) on the activity for N<sub>2</sub> production is probably due to the higher rate of formation of inorganic ad-NO<sub>x</sub> species of the silver phase. It is proposed that these inorganic ad-NO<sub>x</sub> species further react with the reductant or a derived species to form various organo-NO<sub>x</sub> compounds. In particular, organo-nitro and organo-nitroso compounds and/or their derivatives (e.g., isocyanate, cyanide, amines, and NH<sub>3</sub>) are suggested to react with NO or the organo-nitrite and/or its derivative NO<sub>2</sub> to yield N<sub>2</sub>.

When no reductant is present, the 1.2% Ag/ $\gamma$ -Al<sub>2</sub>O<sub>3</sub> material is poisoned by strongly bound nitrates and its activity for NO<sub>2</sub> formation is similar to that observed over the alumina. A material with a high loading of silver (i.e.,

10 wt%) on the alumina displays significantly different catalytic properties as compared to that of a low-loading material; those are probably associated with a metallic state of the silver in the former case and result in the formation of mostly N<sub>2</sub>O at low temperatures during the C<sub>3</sub>H<sub>6</sub>-SCR of NO.

### ACKNOWLEDGMENTS

Part of this project was funded by the European Community, through the Environment and Climate Programme, subprogramme "Technologies for Rehabilitating the Environment." Contracts E5V5-CT94 and ENV4-CT97-0658 and by Forbairt, Contract SC/1997/519. The referees are gratefully acknowledged for their comments on gas-phase reactions.

### REFERENCES

1. Farrauto, R. J., Ed. *Appl. Catal. B* **10**, 1 (1996).
2. Fritz, A., and Pitchon, V., *Appl. Catal. B* **13**, 1 (1997).
3. Burch, R., and Watling, T. C., *Catal. Lett.* **43**, 19 (1997).
4. Burch, R., Fornasiero, P., and Watling, T. C., *J. Catal.* **176**, 204 (1998).
5. Hamada, H., Kintaichi, Y., Inaba, M., Tabata, M., Yoshinari, T., and Tsuchida, H., *Catal. Today* **29**, 53 (1996).
6. Radtke, F., Koepfel, R. A., Minardi, E. G., and Baiker, A., *J. Catal.* **167**, 127 (1997).
7. Miyadera, T., *Appl. Catal. B* **2**, 199 (1993).
8. Okazaki, N., Tsuda, S., Shiina, Y., and Tada, A., *Chem. Lett.* 51 (1998).
9. Yan, J., Kung, M. C., Sachtler, W. M. H., and Kung, H. H., *J. Catal.* **172**, 178 (1997).
10. Yan, J. Y., Kung, H. H., Sachtler, W. M. H., and Kung, M. C., *J. Catal.* **175**, 294 (1998).
11. Bethke, K. A., and Kung, H. H., *J. Catal.* **172**, 93 (1997).
12. Haneda, M., Kintaichi, Y., Inaba, M., and Hamada, H., *Appl. Surf. Sci.* **121**, 391 (1997).
13. Kung, M. C., Bethke, K. A., Yan, J., Lee, J. H., and Kung, H. H., *Appl. Surf. Sci.* **121**, 261 (1997).
14. Sumiya, S., He, H., Abe, A., Takezawa, N., and Yoshida, K., *J. Chem. Soc., Faraday Trans.* **94**, 2217 (1998).
15. Okazaki, N., Tsuda, S., Shiina, Y., Tada, A., and Iwamoto, M., *Chem. Lett.* 429 (1998).
16. Hamada, H., Haneda, M., Kakuta, N., Miura, H., Inami, K., Nanba, T., Hua, W. Q., Ueno, A., Ohfune, H., and Udagawa, Y., *Chem. Lett.* 887 (1998).
17. Nakatsuji, T., Yasukawa, R., Tabata, K., Ueda, K., and Niwa, M., *Appl. Catal. B* **17**, 333 (1998).
18. Shimizu, K., Maeshima, H., Satsuma, A., and Hattori, T., *Appl. Catal. B* **18**, 163 (1998).
19. Meunier, F. C., Breen, J. P., and Ross, J. R. H., *Chem. Comm.* **3**, 259 (1999).
20. Radtke, F., Koepfel, R. A., Minardi, E. G., and Baiker, A., *J. Catal.* **167**, 127 (1997).
21. Schraml-Marth, M., Wokaun, A., and Baiker, A., *J. Catal.* **138**, 306 (1992).
22. Kijlstra, W. S., Brands, D. S., Poels, E. K., and Blik, A., *J. Catal.* **171**, 208 (1997).
23. Cross, A. D., "Introduction to Practical IR Spectroscopy." Butterworth, London, 1964.
24. Colthup, N. B., Daly, L. H., and Wiberley, S. E., "Introduction to Infrared and Raman Spectroscopy." Academic Press, Boston, 1990.
25. Busca, G., Lamotte, J., Lavalley, J. C., and Lorenzelli, V., *J. Am. Chem. Soc.* **109**, 5197 (1987).
26. Nakamoto, K., "Infrared and Raman Spectra of Inorganic and Coordination Compounds," 4th ed. Wiley-Interscience, New York, 1986.
27. Mathyshak, V. A., and Krylov, O. V., *Catal. Today* **25**, 1 (1995).
28. Shimizu, K., Kawabata, H., Satsuma, A., and Hattori, T., *Appl. Catal. B* **19**, L87 (1998).
29. Ukisu, Y., Miyadera, T., Abe, A., and Yoshida, K., *Catal. Lett.* **39**, 265 (1996).
30. Bamweda, G. R., Obuchi, A., Ogata, A., and Mizuno, K., *Chem. Lett.* 2109 (1994).
31. Tanaka, T., Okuhara, T., and Misono, M., *Appl. Catal. B* **4**, L1 (1994).
32. Smits, R., and Iwasawa, Y., *Appl. Catal. B* **6**, L201 (1995).
33. Yokoyama, C., and Misono, M., *J. Catal.* **150**, 9 (1994).
34. Yamaguchi, M., *J. Chem. Soc., Faraday Trans.* **93**, 3581 (1997).
35. Cowan, A. D., Cant, N. W., Haynes, B. S., and Nelson, P. F., *J. Catal.* **176**, 329 (1998).
36. Obuchi, A., Ogata, A., Mizuno, K., Ohi, A., Nakamura, M., and Ohuchi, H., *J. Chem. Soc., Chem. Commun.* 247 (1992).
37. Otsuka, K., Takahashi, R., Amakawa, K., and Yamanaka, I., *Catal. Today* **45**, 23 (1998).
38. Smith, J., Phillips, J., Graham, A., Steele, R., Redondo, A., and Coons, J., *J. Phys. Chem. A* **101**, 9157 (1997).
39. Zuzaniuk, V., Meunier, F. C., and Ross, J. R. H., *J. Chem. Soc., Chem. Comm.* 815 (1999).
40. Cant, N. W., Cowan, A. D., Doughty, A., and Nelson, P. S., *Catal. Lett.* **46**, 212 (1997).
41. Lombardo, E. A., Sill, G. A., d'Itri, J. L., and Hall, W. K., *J. Catal.* **173**, 440 (1998).
42. Obuchi, A., Wogerbauer, C., Koppel, R., and Baiker, A., *Appl. Catal. B* **19**, 9 (1998).
43. Bosch, H., and Janssen, F., *Catal. Today* **2**, 369 (1988).
44. Centi, G., Galli, A., and Perathoner, S., *J. Chem. Soc., Faraday Trans.* **92**, 5129 (1996).
45. Pognant, F., Saussey, J., Lavalley, J. C., and Mabilon, G., *Catal. Today* **29**, 93 (1996).
46. Ueda, A., Ejima, K., Azuma, M., and Kobayashi, T., *Catal. Lett.* **53**, 73 (1998).
47. Burch, R., and Watling, T. C., *Appl. Catal. B* **11**, 207 (1997).